

Supplemental material

Hernandez et al., <https://doi.org/10.1084/jem.20182295>

| | |
|---|--|
| Consensus | AAGAA CAACCA-----AGAACTAGACTTTGTACATAGAACAAA |
| T Sequences | 1037010380103901040010410104201043010440104501046010470 |
| 102_84 consensus | AGGAAT AACC GGGATACAAA CCACGGGT GGA GAACCGGACT CCCCA CAACCT GAAACCGGGAT ATAA CCACGGCT GGAGAACCGGACT CCGCACTT AAAAT GAA |
| YF 993F013Z | AGGAAT AACC GGGATACAAA CCACGGGT GGA GAACCGGACT CCCCA CAACCT GAAACCGGGAT ATAA CCACGGCT GGAGAACCGGACT CCGCACTT AAAAT GAA |
| RNA_2882_Parc NS5_3UTR | AGGAAT AACC GGGATACAAA CCACGGGT GGA GAACCGGACT CCCCA CAACCT GAAACCGGGAT ATAA CCACGGCT GGAGAACCGGACT CCGCACTT AAAAT GAA |
| Yellow fever virus strain BeH655417_JF9 | AAGAA CAAT CA-----AGAACTAGACTTTGTACATAGAACAAA |
| Yellow fever virus strain BeAR646536_JF | AAGAA CAACCA-----AGAACTAGACTTTGTACATAGAACAAA |
| Yellow fever virus strain BeH622205_JF9 | AAGAA CAACCA-----AGAACTAGACTTTGTACATAGAACAAA |
| Yellow fever virus strain BeH622493_JF9 | AAGAA CAACCA-----AGAACTAGACTTTGTACATAGAACAAA |

Figure S1. **Evidence of YFV virus infection in P2.** Sanger sequencing alignments demonstrating an identical insertion in the YFV genome recovered from P2 during her infection. The consensus WT YFV sequence is shown in the top row, while two YFV-17D strains (102_84 and YF993FV013Z) sequenced are directly below that, followed by the sequence from the YFV isolated from the patient (RNA_2882). Environmental YFV isolates are shown in the bottom four rows.

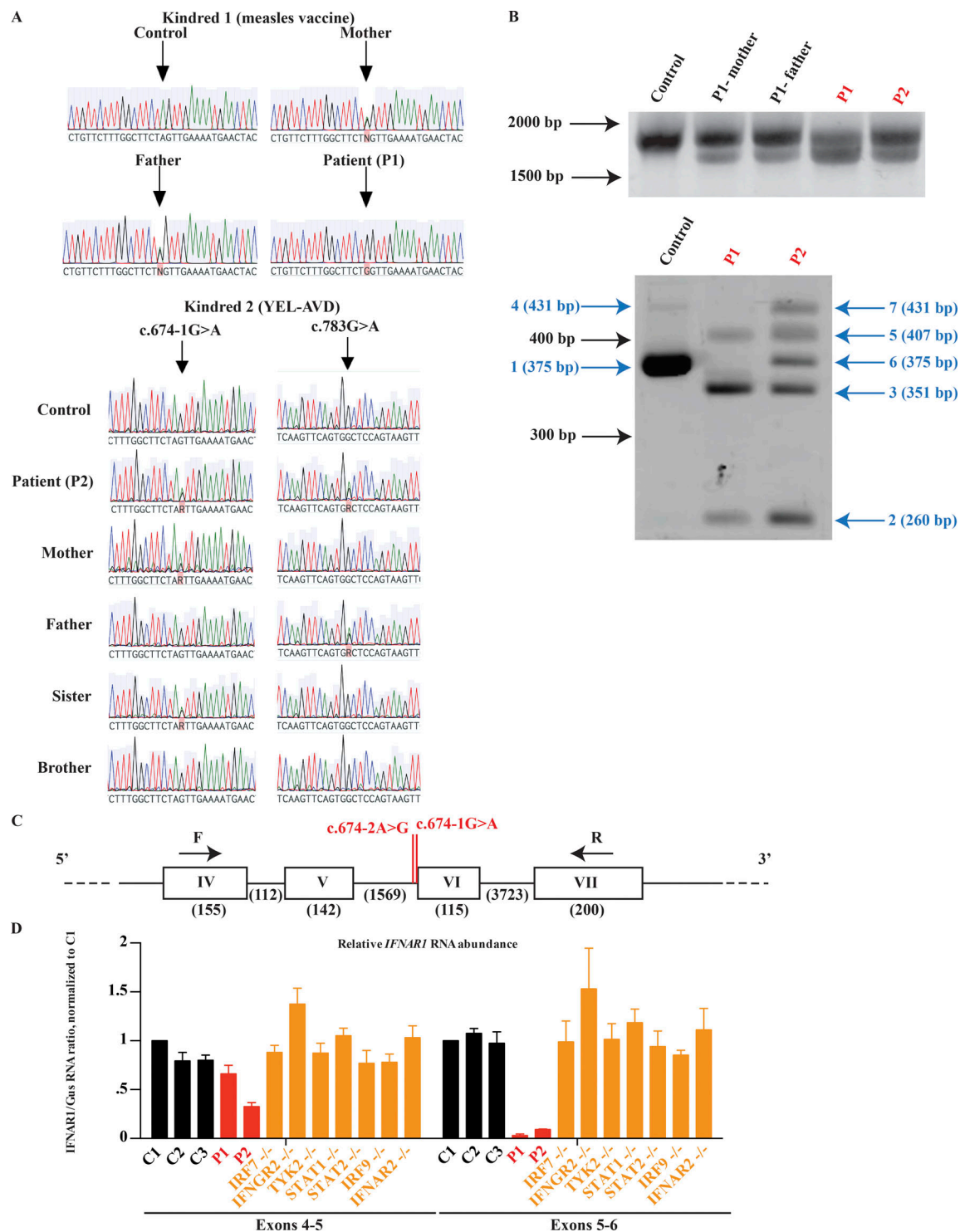


Figure S2. **Genetic analysis of IFNAR1-deficient patients.** (A) Sanger sequencing chromatograms demonstrating c.674-2A>G, c.674-1G>A, and c.783G>A mutations in patient DNA (black arrows). (B) Agarose gel electrophoresis of *IFNAR1* cDNA products generated from patient mRNA transcripts. The upper image shows subtle changes in the size of the full-length transcript (expected length of 1,674 base pairs), while the bottom image demonstrates that additional alternatively spliced mRNAs can be detected at low abundances when only exons IV through VII are amplified, as depicted schematically in C. Numbers in blue correspond to the structure of the transcripts present in a given band, as diagrammed in Fig. 2 A, with nucleotide lengths in parentheses. Representative image from two experiments. (C) Diagram of the *IFNAR1* gene in the region containing exon 6. Exons are depicted with boxes, while introns are depicted with lines. mRNA transcripts from this region were amplified by PCR and inserted into the pGEM-T Easy system. Mutations present in patient cells are indicated with vertical red lines. Primers used in cDNA sequencing are demonstrated (forward, 5'-ATAGCTTAGTTATCTGGAAAACTCTCAGGTG-3'; reverse, 5'-GGGTAGTTT TGACATTTTCACAGTCAGG-3'), and the nucleotide lengths of the features are shown in parentheses. (D) qRT-PCR measuring *IFNAR1* mRNA levels in SV40-F cells from P1, P2, three healthy controls (C1, C2, and C3), *IRF7*^{-/-}, *IFNGR2*^{-/-}, *TYK2*^{-/-}, *STAT1*^{-/-}, *STAT2*^{-/-}, *IRF9*^{-/-}, and *IFNAR2*^{-/-} patients. *IFNAR1*/GUS mRNA ratios are shown after normalization to C1. Mean ($n = 3$) and SEM are shown.

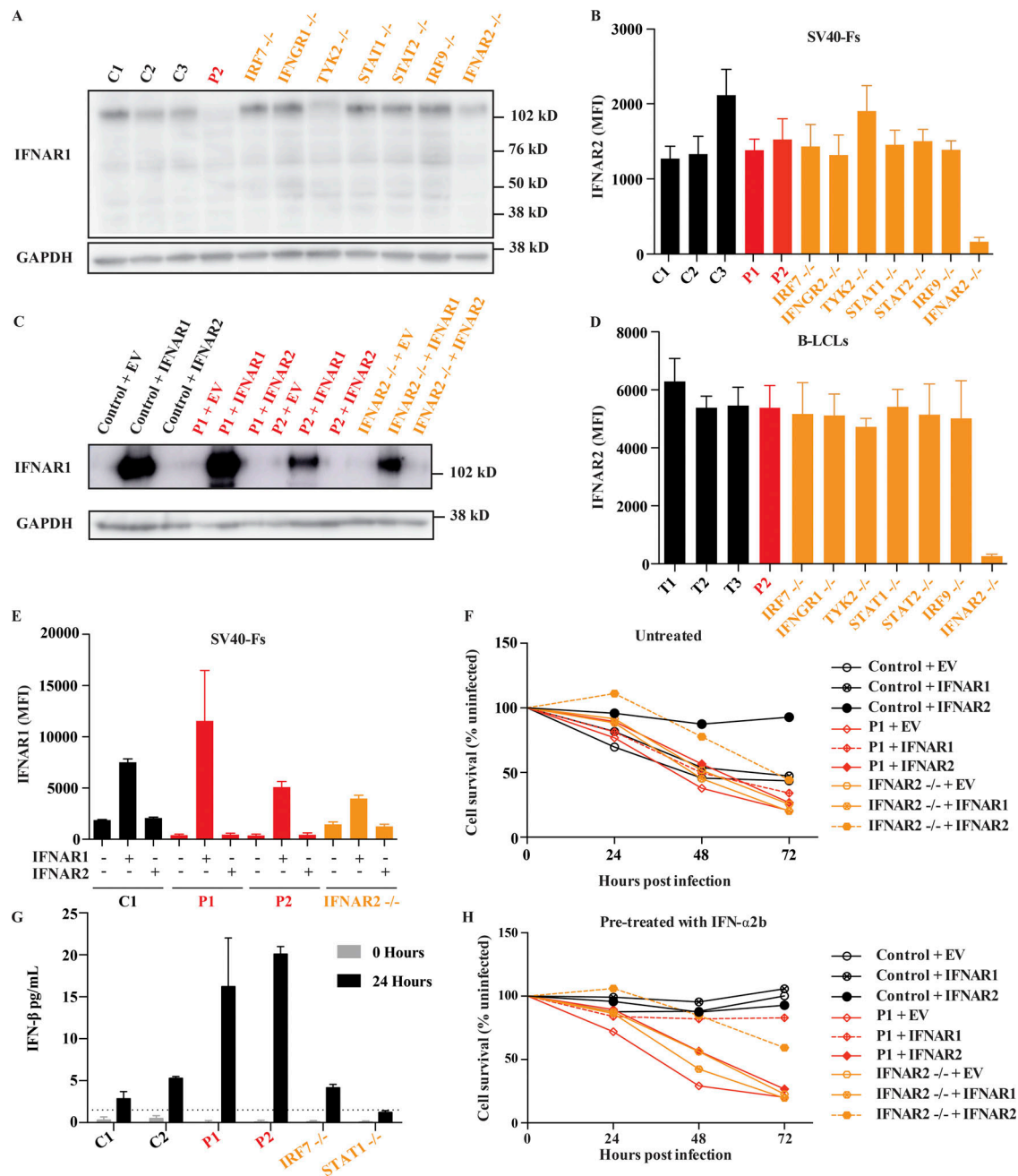


Figure S3. Disrupted function of the type I IFN signaling pathway in patient cells. (A) Western blot of endogenous IFNAR1 in B-LCL cells from three healthy controls (T1, T2, and T3), P2, IRF7^{-/-}, IFNGR1^{-/-}, TYK2^{-/-}, STAT1^{-/-}, STAT2^{-/-}, IRF9^{-/-}, and IFNAR2^{-/-} patients; GAPDH was used as a loading control. A representative blot from three experiments is shown. **(B and D)** IFNAR2 mean fluorescence intensities (MFI) from patient SV40-F (B) and B-LCL (D) cells stained with an anti-IFNAR2 fluorescent antibody. Cells were from three healthy controls (C1, C2, and C3 or T1, T2, and T3), P1, P2, IRF7^{-/-}, IFNGR1^{-/-}, TYK2^{-/-}, STAT1^{-/-}, STAT2^{-/-}, IRF9^{-/-}, and IFNAR2^{-/-} patients and were assessed by flow cytometry. Mean (n = 3) and SEM are shown. **(C)** Western blot of IFNAR1 in SV40-F cells from a healthy control, P1, P2, and an IFNAR2^{-/-} patient transduced with WT IFNAR1, WT IFNAR2, or EV; GAPDH was used as a loading control. A representative blot from two experiments is shown. **(E)** MFIs of SV40-Fs from a healthy control, P1, P2, and an IFNAR2^{-/-} patient and transduced with WT IFNAR1, WT IFNAR2, or EV and stained with an anti-IFNAR1 antibody. Mean (n = 3) and SEM are shown. **(F and H)** Survival rates following VSV infection of primary fibroblasts either untreated (F) or pretreated (H) with 1,000 U/ml IFN-α2b for 24 h before infection. Cells were from a healthy control, P1, and an IFNAR2^{-/-} patient that were either transduced with EV, WT IFNAR1 (IFNAR1), or WT IFNAR2 (IFNAR2). Mean (n = 3) is shown. **(G)** IFN-β levels detected in the supernatant of SV40-F cells either 0 or 24 h after infection with YFV-17D. Cells from two healthy controls (C1 and C2), P1, P2, an IRF7^{-/-} patient, and a STAT1^{-/-} patient were included. The limit of quantitation is indicated by a dotted line. Mean (n = 2) and range are shown.

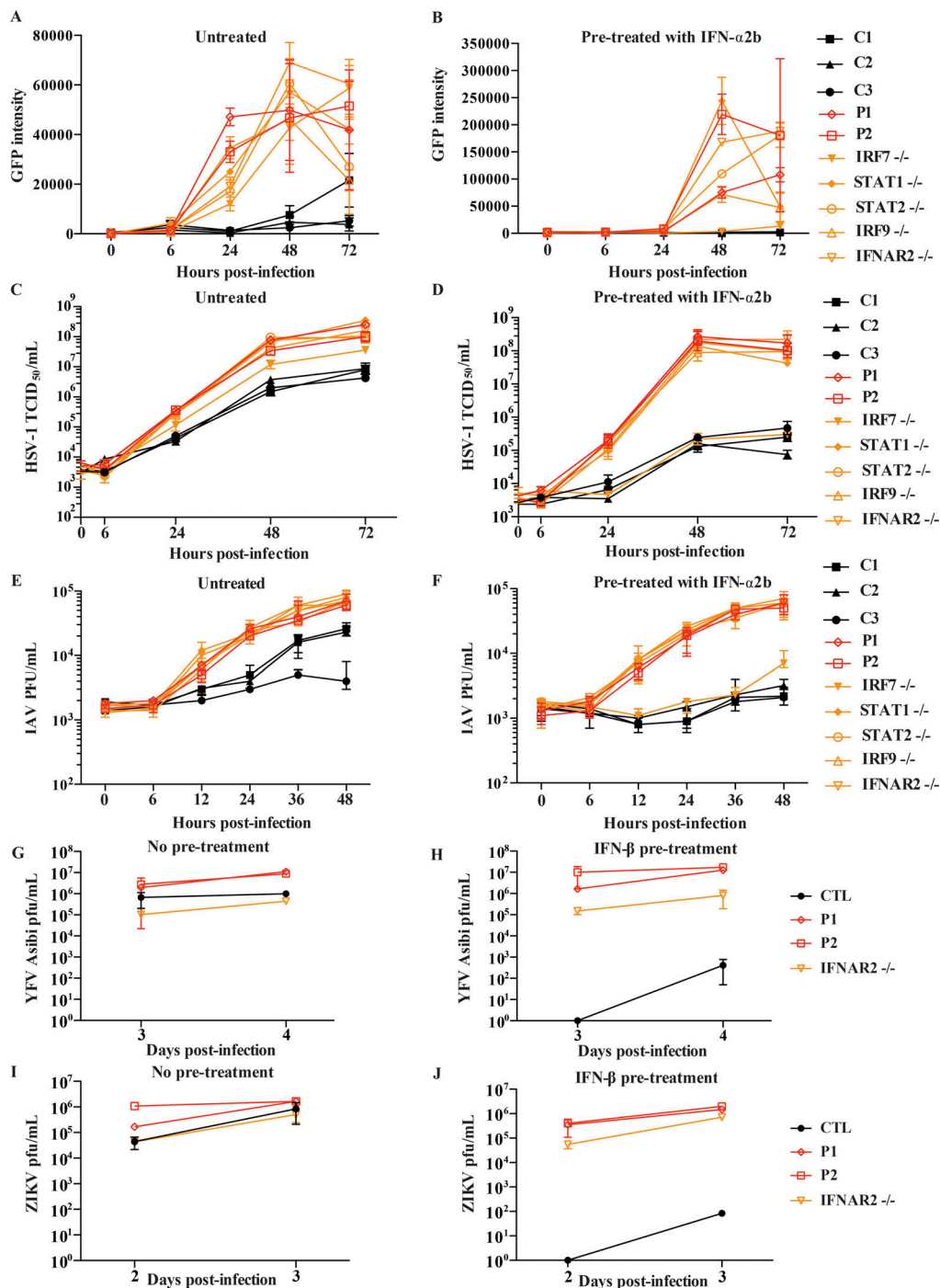


Figure S4. **IFNAR1 is essential for type I IFN-mediated intrinsic immunity to multiple viruses.** (A and B) HSV-1-GFP replication levels, as assessed by GFP intensity, in SV40-F cells unstimulated (A) or pretreated (B) with 1,000 U/ml IFN- α 2b followed by infection with HSV-1-GFP (MOI = 0.01). Cells from three healthy controls were included (C1, C2, and C3), as well as those from P1, P2, IRF7^{-/-}, STAT1^{-/-}, STAT2^{-/-}, IRF9^{-/-}, and IFNAR2^{-/-} patients. Mean ($n = 2$) and range are shown. (C and D) HSV-1 titers in SV40-F cells unstimulated (C) or pretreated (D) with 1,000 U/ml IFN- α 2b for 16 h, followed by infection with HSV-1 (MOI = 0.01). Mean and range ($n = 2$) are shown. Cells from three healthy controls were included (C1, C2, and C3), as well as those from P1, P2, IRF7^{-/-}, STAT1^{-/-}, STAT2^{-/-}, IRF9^{-/-}, and IFNAR2^{-/-} patients. (E and F) IAV titers in SV40-F cells unstimulated (E) or pretreated (F) with 1,000 U/ml IFN- α 2b for 16 h, followed by infection with (A/H1N1/CA/2009) IAV at MOI = 1. Cells from three healthy controls were included (C1, C2, and C3), as well as those from P1, P2, IRF7^{-/-}, STAT1^{-/-}, STAT2^{-/-}, IRF9^{-/-}, and IFNAR2^{-/-} patients. Mean ($n = 2$) and range are shown. (G and H) SV40-F cells stimulated for 16 h with 1,000 U/ml IFN- β before infection (H) or left untreated (G) were infected with 100 μ l of YFV Asibi, and viral titer was assessed by plaque assay on Huh7.5 cells at the given time points. Mean and range ($n = 2$) are shown. Different time points represent independent infections. SV40-Fs from a healthy control, P1, P2, and an IFNAR2^{-/-} patient were included. (I and J) SV40-F cells stimulated for 16 h with 1,000 U/ml IFN- β before infection (J) or left untreated (I) were infected with ZIKV (MOI = 0.05), and viral titer was assessed by plaque assay on Vero cells at the given time points. Mean and range ($n = 2$) are shown. Different time points represent independent infections. SV40-Fs from a healthy control, P1, P2, and an IFNAR2^{-/-} patient were included. TCID, tissue culture infectious dose.

Table S1. **Rare homozygous or possible compound heterozygous variants found by exome sequencing of P1 and P2**

| P1 | P2 |
|--|--|
| URI1 (c.840_842delTGA) | KCNN3 (c.G1092C) |
| CNTF (c.T101A, c.T494G) | KIAA1875-WDR97 (c.3123+1G>T, c.4750G>A) |
| SLC45A1 (c.130_131insCGGGAGATG) | MADCAM1(c.736_737insAGGAG) |
| HTR2B (c.T848C) | IFNAR1 (c.674-1G>A, c.G783A)^{a,b} |
| MTMR9 (c.T1153A) | PIWIL3 (c.A2629C, c.A1996G) |
| PSG11 (c.G44C) | |
| MEOX2 (c.228_230delTGG) ^b | |
| CLN8 (c.A806T) | |
| CNDP1 (c.43_44insTGC) | |
| MPRIIP (c.534_539delCAGCAG) | |
| TMEM247 (c.382_383insAGCGGCAGCACGAGGTGGTGATGGAGCAGCTGCAGCGGG) | |
| FADS6 (c.17_18insGATGGAACCTACGGAGCCCATGGAACCTACGGAGCCCATGGAACCTACGGAGCC) | |
| KIAA2018 (c.4410_4418delTGCTGCTGC) | |
| ZNF407 (c.A515T, c.C4145T) | |
| SMPD1 (:c.108_113delGTCGGC) ^b | |
| TBL1Y (c.G274A) | |
| AOX1 (c.G173A) | |
| BSN (c.G11015A) | |
| MAP3K4 (c.3566_3568delCTG) ^b | |
| ATG3 (c.920dupT) | |
| KIRREL2 (c.32_34delTCC) | |
| CNTD2 (c.T524A) | |
| ACSL3 (c.G1043A) | |
| MAFA (c.621_623delTTGG) | |
| TMPRSS13 (c.248_262del GGGCTGGAGATGCCT) | |
| DYTN (c.C679T) | |
| THAP11 (c.367_369delCAG) | |
| CXorf23 (c.1727_1728delTA) | |
| TMEM54 (c.G136A) | |
| NLRP10 (c.T752C) | |
| SESTD1 (c.A1310G) | |
| APEX1 (c.953_954delTG) ^b | |
| DLC1 (c.G161T) ^b | |
| PLBD1 (c.74_76delGCA) | |
| ANKRD62 (c.G1197C) | |
| MAML3 (c.1506delG) ^b | |
| RBM23 (c.1077_1078insGCC) | |
| HOXD9 (c.794_795insGCA) ^b | |
| DCP1B (c.782_783insGCA, c.C1532T) | |
| IFNAR1 (c.674-2A>G) ^b | |

Unbolded genes are homozygous, while bolded genes may be compound heterozygous or may occur on the same allele. The consequences of the variations on coding sequences are given in parenthesis following each gene.

^aGene containing a stop-gain mutation.

^bGene that is predicted to be related to primary immunodeficiencies via a connectome analysis ([Itan et al., 2013](#)).

Reference

Itan, Y., S.-Y. Zhang, G. Vogt, A. Abhyankar, M. Herman, P. Nitschke, D. Fried, L. Quintana-Murci, L. Abel, and J.-L. Casanova. 2013. The human gene connectome as a map of short cuts for morbid allele discovery. *Proc. Natl. Acad. Sci. USA*. 110:5558–5563. <https://doi.org/10.1073/pnas.1218167110>